Parameter space representation of liquid crystal display operating modes

H. S. Kwok
Centre for Display Research and Department of Electrical and Electronic Engineering, Hong Kong University of Science and Technology, Clear Water Bay, Hong Kong

(Received 7 May 1996; accepted for publication 26 June 1996)

A parameter space approach is used to represent the operation of all liquid crystal displays. The Jones matrix nematic is used to analyze the static optical properties of liquid crystal displays with any twist angle, cell thickness, natural birefringence, and polarizer angles. All the usual display modes such as 90° TN, ECB, OMI, SBE, and STN can be visualized on a simple parameter space diagram. Besides its pedagogical values, this formulation has the advantage of simplicity in showing the physics and operating conditions of supertwist as well as low twist liquid crystal displays. It can also be used to analyze novel situations such as reflective displays which do not require any back polarizer. © *1996 American Institute of Physics.* [S0021-8979(96)05219-X]

I. INTRODUCTION

Optical modeling of liquid crystal displays (LCD) is an important step in the design of LCDs. One of the more successful techniques for analyzing the optical properties of LCDs is based on the generalized geometric optics approximation (GGOA).[1,2] This theoretical treatment is suitable for the analysis of generalized twisted nematic (GTN) liquid crystal displays which include large as well as low twist angles. It is an improvement over the earlier work of Gooch and Tarry.[3] Lien later extended the GGOA method to a Jones matrix form.[4]

In another approach, the twisted nematic liquid crystal cell can be regarded as a stack of birefringent plates, each twisted slightly from the other.[5] If the number of plates is large enough, then each member can be treated as a simple uniaxial birefringent plate. This stack of plate approximation is similar to a fan Solc filter and can be described by a product of Jones matrices.[5] For the case of constant tilt and uniform twist of the liquid crystal director, an analytic form of the LCD Jones matrix can be obtained. It is interesting to note that the final Jones matrix for the liquid crystal cell derived this way agrees exactly with the GGOA results. For the case of nonuniform twist and tilt of the liquid crystal director, the stack of plates can be solved numerically either using the 2×2 Jones matrix or the more general 4×4 Berreman matrix.[6]

While commercial softwares are available for calculating the optical properties of specific LCDs, it is still desirable to have a quick analysis of the design of different displays before the detailed numerical modeling is made. In particular, it will be extremely useful to visualize the operation of the LCD as a function of various parameters in a single parameter space diagram. All systematic trends can be seen in one diagram without going through many rounds of numerical simulations. In this paper, we show that it is possible to generate such a ''parameter space representation'' of the operation of various kinds of LCDs. This parameter space approach to the solution of LCD optics also has the advantage of providing a clear physical understanding of the various display modes. It can also be used to analyze some novel situations such as reflective GTN displays without any back polarizers.

In this paper, we shall limit ourselves to the systematic study of the static (no voltage) optical properties of GTN liquid crystal displays. Dynamic cases with applied voltages and nonuniform twist and tilt of the director will not be dealt with. These situations cannot be parametrized in the same manner and are more suitably simulated individually using commercial softwares. In this paper, it will be shown that static parameter space diagrams can be generated yielding the operating conditions of GTN that are similar to conventional ECB (electrically controlled birefringence),[7] TN (twisted nematic),[7] STN (supertwisted nematic),[8] SBE (supertwisted birefringence effect),[9] and OMI (optical mode interference)[10] displays. The most important result is that all these display modes can be presented as a GTN in the same parameter space.

For the calculation of the optical properties of GTN at normal incidence, we shall use the generalized Jones matrix method. This 2×2 matrix approach is totally adequate for the present situations. In the following, we shall first present the analytical formulation of the Jones matrix, before the cases of transmissive and reflective LCDs are discussed. This Jones matrix is consistent with the GGOA of Ong,[1,2] and the formulation of Yeh.[5] It is also in agreement with the formulas presented by Lien.[4]

II. THE JONES MATRIX

The parameter space diagrams of the GTN LCD are generated using the Jones matrix. The most important point to note is that the twist angle of the liquid crystal director is assumed to be uniform and the tilt angle is assumed to be constant over the entire cell. These assumptions, of course, are not valid for the cases of an applied voltage above the threshold value. Even for the zero volt case, it is well-known that the tilt angle decreases in the middle of the liquid crystal cell due to elastic energy minimization, especially for high pretilt cases.[10] However, as pointed out by Lien,[4] even in the high pretilt case, an average tilt angle can be used without producing any significant error in predicting the properties of the LCD. In this paper, we shall assume that the tilt angle is

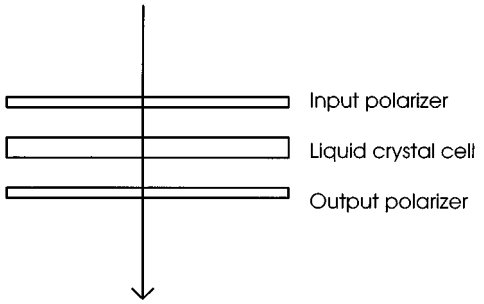

FIG. 1. Optical arrangement for a transmission type LCD.

constant throughout the LC cell. As a matter of fact, to simplify the discussions further, we shall use a pretilt angle of 0° in this paper.

The Jones matrix for the LC cell is given by

$$M=\begin{pmatrix} A-iB & -C-iD \\ C-iD & A+iB \end{pmatrix}, \tag{1}$$

where

$$A=\cos\ \phi\ \cos\ \beta d+\frac{\phi}{\beta d}\sin\ \phi\ \sin\ \beta d, \tag{2}$$

$$B=\frac{k_a}{\beta}\cos\ \phi\ \sin\ \beta d, \tag{3}$$

$$C=\sin\ \phi\ \cos\ \beta d-\frac{\phi}{\beta d}\cos\ \phi\ \sin\ \beta d, \tag{4}$$

$$D=\frac{k_a}{\beta}\sin\ \phi\ \sin\ \beta d. \tag{5}$$

In Eqs. (2)–(5), ϕ and d are the twist angle and thickness of the LC cell, respectively, and

$$\beta d=(k_a^2 d^2+\phi^2)^{1/2}, \tag{6}$$

$$k_a=\pi\Delta n/\lambda, \tag{7}$$

where

$$\Delta n=n_e(\theta)-n_0, \tag{8}$$

is the birefringence of the tilted liquid crystals and $n_e(\theta)$ is the extraordinary index at an average director tilt angle of θ and is given by the usual expression

$$\frac{1}{n_e^2(\theta)}=\frac{\cos^2\ \theta}{n_e^2}+\frac{\sin^2\ \theta}{n_0^2}. \tag{9}$$

As explained above, we shall assume θ to be zero in this paper. Hence, $\Delta n=n_e-n_0$ always. At any wavelength λ, the Jones matrix is completely defined once ϕ and $d\Delta n$ are given. In the following sections, we shall examine the static parameter space (ϕ and $d\Delta n$) for the transmission or reflection of a LCD under zero voltage bias.

III. TRANSMISSIVE LCD WITH 0° POLARIZER

In a simple transmissive LCD, a liquid crystal cell is placed between 2 polarizers as shown in Fig. 1. The input

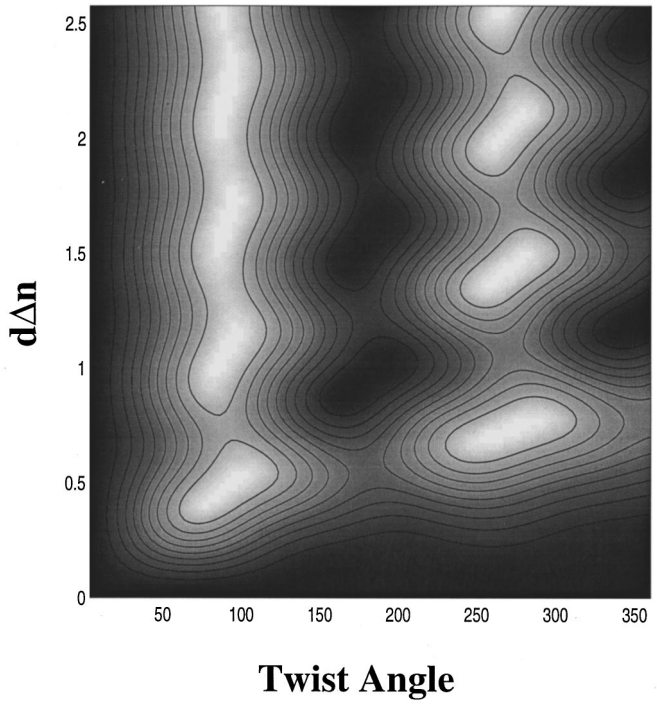

FIG. 2. Contour map of the transmission of the LCD as a function of $d\Delta n$ and ϕ. The polarizer angle is 0°. The successive contours are in steps of 10%.

and output polarizer axes are at an angle of α and γ to the input director of the liquid crystal cell, respectively. This geometry is essentially the same as in GGOA.[1] The transmission of this optical arrangement is given by

$$T=\left|(\cos\ \gamma\ \sin\ \gamma)\cdot M\cdot\begin{pmatrix}\cos\ \alpha\\ \sin\ \alpha\end{pmatrix}\right|^2. \tag{10}$$

For the case of $\alpha=0°$ and $\gamma=\phi+\pi/2$, it can be shown that Eq. (10) leads to the familiar expression of Gooch and Tarry:[3]

$$T=\frac{1}{1+u^2}\sin^2\ \phi\sqrt{1+u^2} \tag{11}$$

where $u=\pi d\Delta n/\lambda\phi$.

If we consider the simple situation where the display operates between a voltage of zero and a high value such that the LC becomes homeotropic, then it makes more sense to let $\gamma=\alpha+\pi/2$ or $\gamma=\alpha$ instead of $\gamma=\phi+\pi/2$. In such cases, the high voltage homeotropic state of the LC cell will have a transmission of either 0% or 100% depending on whether the polarizers are crossed or parallel. As we have mentioned previously, such assumptions may not be practical for multiplexed passive matrix displays. In those cases, both the select and nonselect states have finite voltages. The LC alignment is never truly in the homeotropic state and there is always some residual twist and tilt.[11,12] However, for the purpose of our discussions here, those effects will not be considered. In the following, we shall assume that $\gamma=\alpha+\pi/2$ which corresponds to the case of normally bright operation.

Figure 2 shows a contour plot of the transmission of the GTN LCD with ϕ and $d\Delta n$ as the independent variables at $\lambda=550$ nm and $\alpha=0°$. The contour lines are in steps of 10%

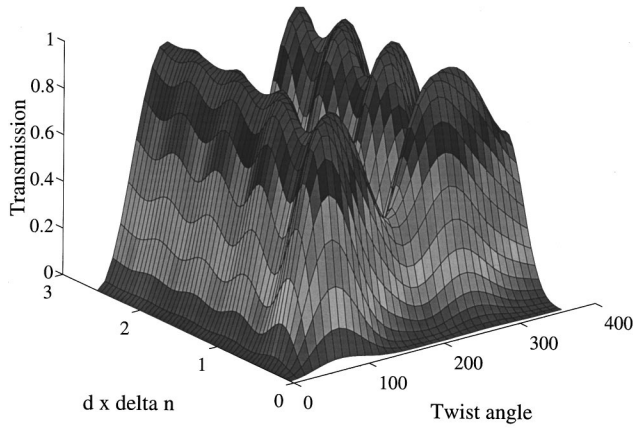

FIG. 3. Same result as Fig. 2 shown in a 3D plot.

increment in transmission. Shading is provided to distinguish better the peaks and the valleys. The x-axis corresponds to $d\Delta n=0$ or no liquid crystal cell. Hence, $T=0\%$. Similarly, the y-axis corresponds to $\phi=0°$ or a retardation plate with the optical axis parallel to the polarizer. Hence, $T=0\%$ as well. Figure 3 is a 3D plot of the same result. These figures represent the solution space of the transmissive LCD for all combinations of with ϕ and $d\Delta n$. It is essentially the parameter space for the GTN. The usual diagrams of T vs d or T vs $d\Delta n$[1–4] are simply vertical cuts of this diagram for each particular twist angle ϕ.

Several interesting features can be observed in Fig. 2. First of all, the case of 90° TN display is clearly shown in that figure. 90° TN corresponds to the vertical line of $\phi=90°$ in Fig. 2 or the mountain ridge in Fig. 3. The top curve in Fig. 4 shows the dependence of T on $d\Delta n$. It depicts all the classic Mauguin behavior with the first minimum at $d\Delta n=0.5$ μm, the second minimum at $d\Delta n=1.1$ μm etc.[1,3] It should be noted that the Mauguin minima usually refer to a parallel/parallel polarizer geometry. They actually correspond to the maxima in our present situation. We shall keep referring to them as ''minima'' in accordance with common practice.

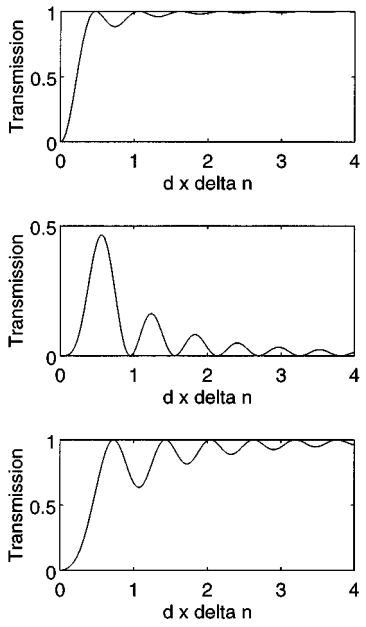

FIG. 4. Transmission of the 90° (top), 180° (middle), and 270° (bottom) displays as a function of $d\Delta n$ for $\alpha=0°$. Waveguiding or adiabatic limit exists in all cases.

In Fig. 2, there is another set of solutions with 100% transmission at $\phi=270°$. The first and second ''Mauguin minima'' for this set of solutions have $d\Delta n$ values of 0.75 and 1.5 μm, respectively. They are similar to the SBE mode of Scheffer and Nehring.[7] There is an important distinction between the normal SBE modes and the present SBE-like solution. The SBE display as originally suggested has $\alpha=-32.5°$ and $\gamma=32.5°$ while here, $\alpha=0°$ and $\gamma=90°$ because of the assumption of the voltages used. Moreover, the pretilt angle for the SBE display in Ref. 9 is 28°. That accounts for the peculiarly optimized polarizer angles in their paper. The values of α and γ for the SBE-like mode as depicted in Fig. 2 can in principle be optimized further to produce practical displays.

In Fig. 2, there is also a series of saddle points at $\phi=180°$, with $d\Delta n$ values of 0.55 μm, 1.25 μm, etc. These are very similar to the literature OMI modes.[8] In this case, the OMI-like modes in Fig. 2 and the actual OMI modes are quite similar. The polarizer angles and $d\Delta n$ values are comparable. As in the OMI modes, the peak transmission in the first saddle point (on-state) is only about 45%. It is even smaller for the other saddle points along $\phi=180°$.

Figure 4 shows the transmission of the LCD as a function of $d\Delta n$ for the 3 cases discussed: 90°, 180°, and 270°. It can be seen that there are a series of Mauguin minima in all cases, followed by the waveguiding or adiabatic limit. That is, if $d\Delta n$ is large enough, the transmission eventually approaches a constant which is independent of $d\Delta n/\lambda$. This is the most desirable operating mode for the TN and SBE-like modes. But for the OMI-like solution, waveguiding implies that the polarization of the output light is rotated by 180° relative to the input. Thus, there is no change in the polarization at all. So this operating mode has to rely on the finite transmission between the ''Mauguin minima,'' or the saddle points in Fig. 2.

Figure 5 shows the dispersion of the first operating points for the TN, OMI, and SBE-like modes, respectively. Actually wavelength dispersion of any operating point can be observed qualitatively from Fig. 2. Since the wavelength λ enters the equation through the term $d\Delta n/\lambda$, a change in λ is the same as a change in $d\Delta n$, or a vertical shift of the operating point in Fig. 2, or along the x-axis in Fig. 4. It can be seen that as expected, the TN display has almost no wavelength dependence.

IV. TRANSMISSIVE LCD WITH 45° POLARIZER

Figure 6 shows the parameter space for the case of $\alpha=45°$, again with shadings to indicate the peaks and valleys of the solution space more clearly. Here, there are even more operating points where the transmission is 100% than shown in Fig. 2. First, the 90° TN modes and the SBE-like modes at 270° are still present. We can call them the TN′ and SBE′ modes since they are like the TN and SBE modes with the

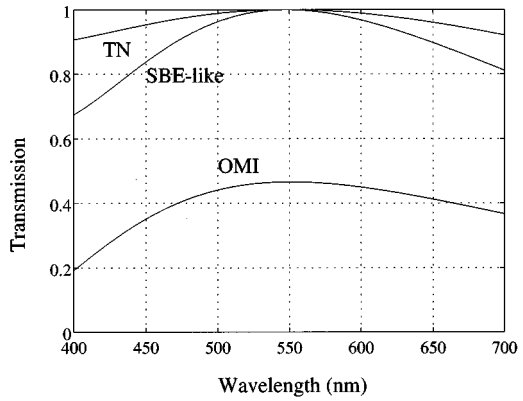

FIG. 5. Dispersion of the transmission for the LCD in 3 different operating points: (a) 90° TN, $\phi=90°$, $d\Delta n=0.5$ μm, (b) SBE-like, $\phi=270°$, $d\Delta n=0.72$ μm, and (c) OMI-like $\phi=180°$, $d\Delta n=0.56$ μm.

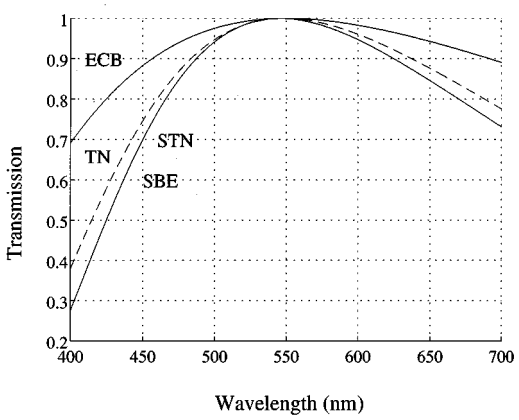

FIG. 7. Dispersion of the transmission for the LCD in 4 different operating points: (a) ECB, $\phi=0°$, $d\Delta n=0.275$ μm, (b) TN′, $\phi=90°$, $d\Delta n=0.475$ μm, (c) STN-like, $\phi=180°$, $d\Delta n=0.61$ μm, and (d) SBE′, $\phi=270°$, $d\Delta n=0.74$ μm. The last 2 curves overlap exactly.

wrong polarizer orientation. In addition to these solutions, there are 2 more sets of solutions at $\phi=0°$ and 180°.

The 0° solution is exactly the ECB mode.[7] The LC cell has no twist and is exactly in a homogeneous alignment. It can be shown from Eq. (10) that the transmission of the LCD is given by the periodic function[7]

$$T=\sin^2\ \pi d\Delta n/\lambda. \tag{12}$$

This is exactly as depicted in Fig. 6. This shows the advantage of a parameter space presentation in Figs. 2 and 6, that all the modes are succinctly displayed on one graph. It is easy to see what happens to the display if the operating conditions are slightly different from the exact design.

The set of solutions at $\phi=180°$ is similar to the OMI mode in Fig. 2, except that now the peak transmissions are 100% instead of a much lower value. These are actually very similar to the normal 180° STN modes.[8] Even the polarizer angles are the same. As in the ECB mode, this STN mode is also quite dispersive. Figure 7 shows the dispersion curves for the first operating points (the first ''Mauguin minima'') of the ECB, TN′, STN, and the SBE′ modes. It can be seen that they are more dispersive than the $\alpha=0°$ cases in Fig. 5.

The major difference between the $\alpha=0°$ and the $\alpha=45°$ cases is that in the latter situation, the LC cell behaves somewhat as a retardation plate and the operating points are more sensitive to the birefringence of the liquid crystal cell. Figure 8 shows the transmission of the 90°, 180°, and 270° displays as a function of $d\Delta n$. It can be seen that an interference

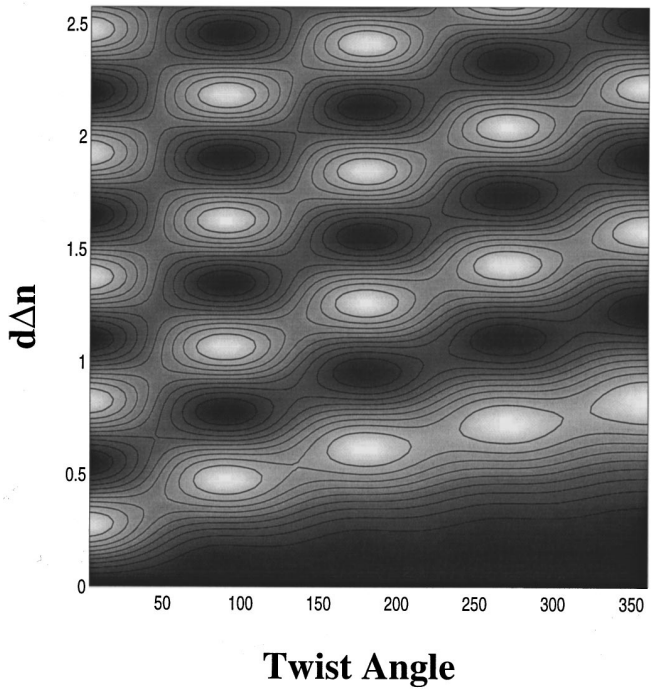

FIG. 6. Contour map of the transmission of the LCD as a function of $d\Delta n$ and ϕ. The polarizer angle is 45°. The successive contours are in steps of 10%.

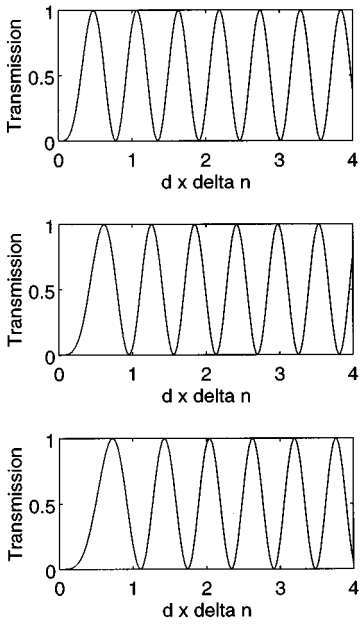

FIG. 8. Transmission of the 90° TN′ (top), 180° STN (middle), and 270° SBE′ (bottom) displays as a function of $d\Delta n$. Interference effects are seen for all values of $d\Delta n$.

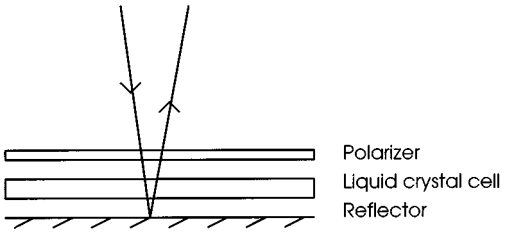

FIG. 9. Optical arrangement for the reflective LCD.

behavior is always present. In this geometry, the waveguiding limit cannot be obtained for any value of ϕ. In other words, the solution of a single linearly polarized light inside the LC cell is no longer possible.

This is quite obvious physically. In the adiabatic limit for large $d\Delta n$, the normal modes of propagation inside the liquid crystal cell are linearly polarized waves with polarization vectors along and perpendicular to the input director.[11] Therefore the $\alpha=0°$ modes in Fig. 2 have only one wave propagating inside the LC cell and will be waveguiding in the adiabatic limit. On the other hand, the $\alpha=45°$ modes always have 2 waves propagating inside the cell which will interfere at the output. They are therefore more aptly described as ''interference modes.''

This fundamental difference between the $\alpha=0°$ and $\alpha=45°$ modes leads to an interesting classification of the different operating modes of a GTN LCD. The $\alpha=0°$ modes have adiabatic or waveguiding limits at large $d\Delta n$ as seen from Fig. 4, while the $\alpha=45°$ modes are more interference in characteristics as shown by Fig. 9. It therefore makes more physical sense to call all $\alpha=0°$ or near 0° displays TN and STN LCD, while calling $\alpha=45°$ or near 45° displays OMI LCD. Using this definition, the ECB display is also one of the OMI modes.

It should be reiterated that in comparing the various operating modes of the transmissive display, we only based our discussions on the static state of the LCD. However, in practical situations, the voltage-on (select) state is not strictly homeotropic, and the residual birefringence, twist, and tilt of the liquid crystals can greatly affect the contrast and viewing angle of the LCD.[12] Moreover, for the case of highly multiplexed STN displays, even the nonselect state should have a voltage. So the 0 V static case will not be strictly correct. In these situations, detailed numerical simulations where $\theta(z)$ and $\phi(z)$ are given by a solution of the Euler equations will then have to be carried out.

V. REFLECTIVE DISPLAYS

The parameter space for the GTN can also be constructed for the case of reflective displays as well. Truly reflective displays are desirable from the manufacturing point of view. The back polarizer can be eliminated, and the rear reflector can be incorporated as part of the LC cell. This will lead to many advantages such as increased brightness and the elimination of shadows. Such displays have been explored by Sonehara *et al.*,[13] and more recently by Fukuda

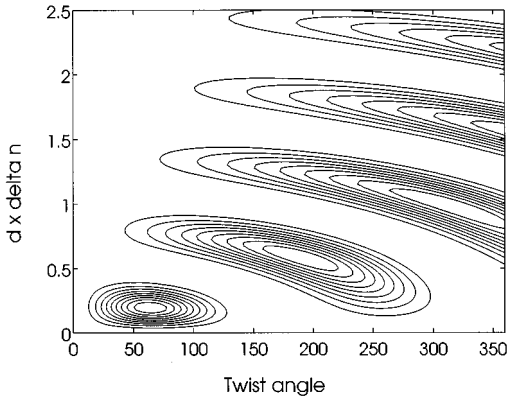

FIG. 10. Contour map of the reflection of the LCD as a function of $d\Delta n$ and ϕ. The successive contours decrease starting from the x-y axes in 10% increment to 10%.

et al.[14] By constructing the parameter space, the physical principles of such reflective displays can be visualized easily.

The geometry for this display is extremely simple. As shown in Fig. 9, the reflective display consists of only an input polarizer, the LC cell and a rear mirror. For this reflective display, it can be assumed that the voltage on state corresponds to a homeotropic alignment, or $R=100\%$. So the idea is to find a combination of ϕ and $d\Delta n$ such that $R=0\%$. That is, for this display to work, the LC cell should behave as a quarter-wave retardation plate, so that the light is cross-polarized upon reflection through the LC cell twice. This is actually similar to an electro-optic Q-switch in a pulsed laser system.[15] Using this argument, the display in Fig. 9 can be analyzed analytically by noting that the ellipticity of the output of a GTN cell is given by[3]

$$\epsilon=\tan\left[\frac{1}{2}\sin^{-1}\left(\frac{2u}{1+u^2}\sin^2\phi\sqrt{1+u^2}\right)\right]. \tag{13}$$

If the LC cell should behave as a quarter-wave plate, then $\epsilon=\pm 1$ and it follows from Eq. (13) that the only solutions are $\phi=(2N-1)\pi/2\sqrt{2}$ and $d\Delta n=(2N-1)\lambda/2\sqrt{2}$, where $N=1,2,3,\ldots$. The first 2 operating points of this reflective display are $(\phi, d\Delta n)=(63.6°, 0.194\ \mu\text{m})$ and $(190.8°, 0.583\ \mu\text{m})$ at $\lambda=550$ nm, respectively. These values agree quite well with the experimental results of Sonehara *et al.*[13]

These solutions can be obtained using the parameter space approach as well, and in a more succinct manner. Using the geometry in Fig. 9, the reflection of the display is given by

$$R=\left|(\cos\alpha\ \sin\alpha)\cdot HMHM\cdot\begin{pmatrix}\cos\alpha\\ \sin\alpha\end{pmatrix}\right|^2, \tag{14}$$

where

$$H=\begin{pmatrix}\cos\phi & \sin\phi\\ \sin\phi & -\cos\phi\end{pmatrix}. \tag{15}$$

Figure 10 is a contour plot of the solution of Eq. (14) with $\alpha=0°$ and using ϕ and $d\Delta n$ as the independent parameters. The reflectivity is 100% along the x-y axes, and decreases by a 10% increment for each contour line. It is essentially the parameter space for the reflective GTN. It can be seen that in

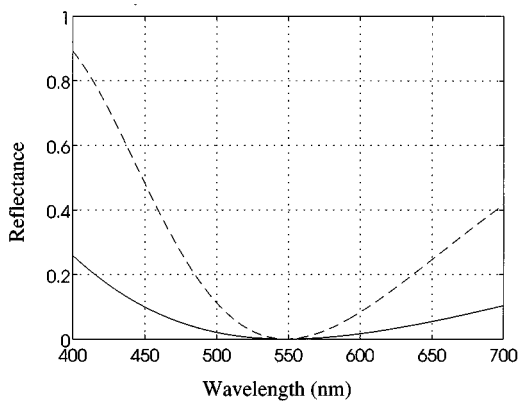

FIG. 11. Dispersion of the reflective LCD in 2 different operating points: (a) $\phi=63.6°$, $d\Delta n=0.194$ μm, (solid line) (b) $\phi=190.8°$, $d\Delta n=0.583$ μm, (dashed line).

the range of parameters used there are several solutions for $R=0\%$ at no applied voltage, and they agree exactly with the analytical results obtained above.

From Fig. 10, it can be seen that this reflective display is rather dispersive. A small change in λ will imply a large change in R. Actually the expected dispersion can be obtained easily with Eq. (14) and is shown in Fig. 11. In Fig. 11, the reflectivity of the first 2 operating points in Fig. 10 are plotted as a function of λ. The result is similar to that of Ong for the low twist transmissive display.[1] Figure 11 shows that the reflective display is more dispersive than the transmission modes in Figs. 5 and 7. Currently, there are some efforts in reducing this color dispersion effect in reflective nematic displays. For example, Fukuda *et al.* proposed the insertion of a retardation film between the polarizer and the liquid crystal cell to reduce the dispersion.[14] We have also recently obtained good black and white reflective displays using a different scheme. Our results in this direction will be reported in a separate publication.[16]

Finally, Fig. 12 shows the reflectivity of this display as a function of $d\Delta n$ for the first 2 dark states in Fig. 10. They are essentially cuts along the $\phi=63.6°$ and 190.8° lines. Interestingly, the behavior of Fig. 12 indicates some sort of waveguiding limit for this reflective display. That is, at large $d\Delta n$, the reflectivity approaches a constant. In this case, the adiabatic limit is equivalent to an empty cell, i.e., 100% reflectivity. It is understandable from the waveguiding point of view. Since $\alpha=0°$, the input linearly polarized light is rotated by ϕ going into the cell, and rotated by $-\phi$ coming out of the cell in the opposite direction. Hence, there is no change in the polarization and the reflectivity is 100%.

It is also possible to generate the $\alpha=45°$ parameter space for the reflective LCD. However, this case will not be discussed further here.

VI. SUMMARY

In summary, we have shown that the parameter space approach is very useful in identifying the operating points and operating modes of the various liquid crystal displays. The parameter space can be easily generated by a Jones matrix calculation. It is shown that many of the common display

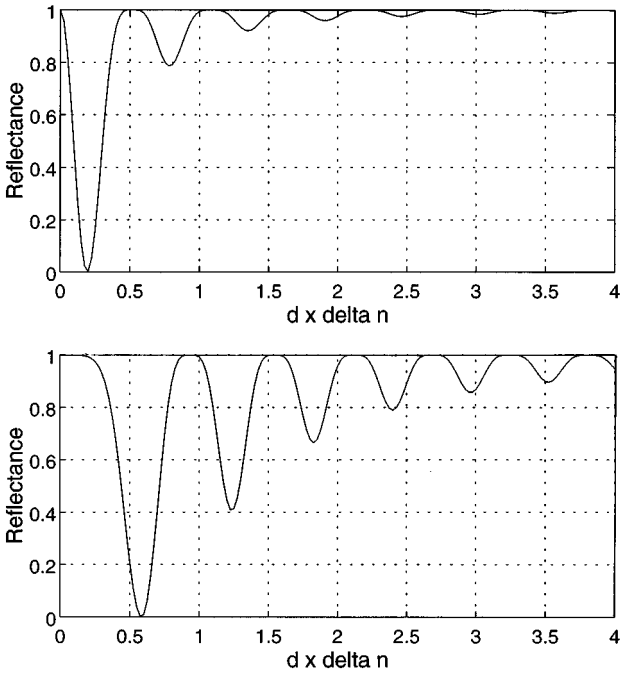

FIG. 12. Reflectance of the 63.6° (top) and 190.8° (bottom) displays as a function of $d\Delta n$. Waveguiding limits are evident.

modes can be predicted and depicted on the same parameter space diagram. This calculation can be of great pedagogical value, as well as being an aid in optimizing the LCD display.

We also showed the fundamental difference between the 2 input polarizer orientations of 0° and 45°. The former always allow waveguiding solutions, while the latter will always lead to interference effects. It is true for both transmissive and reflective displays. We propose a consistent nomenclature of all general twisted nematic displays based on the polarizer angle, rather than based on the twist angle. Input polarizer angles near 0° should belong to one class while those with 45° alignment should be called differently.

It is shown that the parameter space method can be used to analyze reflective displays as well. Again the entire parameter space can be obtained and visualized. The numerical results agree well with analytical solutions for obtaining the operating points. Reflective display is a great simplification over existing displays and has many advantages. If the dispersion effect can be overcome, this reflective display can have many applications potentials.

One obvious advantage of the Jones matrix approach is the ease of modeling displays which incorporate other optical elements such as birefringent films of any retardation value. The parameter space can be readily generated for various arrangements to visualize the operation characteristics of these displays. Further work on such reflective GTN displays is in progress and will be reported separately.

ACKNOWLEDGMENTS

This research was supported by the Hong Kong Industry Department.

[1] H. L. Ong, Proc. SID **29**, 161 (1988).
[2] H. L. Ong, J. Appl. Phys. **64**, 614 (1988).
[3] G. H. Gooch and H. A. Tarry, J. Phys. D **8**, 1575 (1975).
[4] A. Lien, J. Appl. Phys. **67**, 2853 (1990).
[5] P. Yeh, *Optical Waves in Layered Media* (Wiley, New York, 1988).
[6] F. H. Yu, S. T. Tang, J. Chen, and H. S. Kwok (unpublished).
[7] I. C. Khoo and S. T. Wu, *Optics and Nonlinear Optics of Liquid Crystals* (World Scientific, Singapore, 1993).
[8] F. Leenhout, M. Schadt, and H. J. Fromm, Appl. Phys. Lett. **50**, 1468 (1987).
[9] T. J. Scheffer and J. Nehring, J. Appl. Phys. **58**, 3022 (1985).
[10] M. Schadt and F. Leenhouts, Appl. Phys. Lett. **50**, 236 (1987).
[11] P. Allia, C. Oldano, and L. Trossi, in *Physics of Liquid Crystalline State*, edited by I. C. Khoo and F. Simoni (Gordon and Breach, Philadelphia, 1991).
[12] L. M. Blinov and V. G. Chigrinov, *Electrooptic Effects in Liquid Crystal Materials* (Springer, New York, 1994).
[13] T. Sonehara and O. Okumura, Japan Display, Proceedings of the 9th International Display Research Conference, Society for Information Displays, 1989, paper 7-6.
[14] I. Fukuda, M. Kitamura, and Y. Kotani, Asia Display, Proceedings of the 15th International Display Research Conference, Society for Information Displays, 1995, paper P3.5-3.
[15] A. Yariv, *Optical Electronics* (HRW, New York, 1985).
[16] S. T. Tang, M. Wong, and H. S. Kwok (unpublished).